

Military Technical College
Kobry El-Kobbah
Cairo, Egypt



10th International Conference
On Aerospace Sciences &
Aviation Technology

STATOR FAILURES AND DIAGNOSTIC NEURAL-BASED METHODS IN 3-PHASE SQUIRREL-CAGE INDUCTION MOTORS

I.F.El-arabawy^{*}, Ragy^{**}, R. A.A.Nasser^{***}, and Gamal^{****} M.

ABSTRACT

This paper presents the stator winding fault detection. Stator failures are classified. Effect's of various stresses on the stator lifetime and how do causes contribute to stator failure are studied. A technique known as model-based diagnostic technique is used to study the behavior of the stator under abnormal conditions. The squirrel-cage induction motor is taken as a case study for practical verification. A neural-based diagnosis for the stator failures has been carried out. The algorithm has proven adequacy in predicting stator faults.

KEY WORDS

induction motor, squirrel-cage, Signature analysis, Fault detection, Stator faults and Neural Network Application.

* Professor, Dpt. of Electrical Engineering, Alexandria University, Alexandria, Egypt.

** Ph.D., Dpt. of Electrical Engineering, Alexandria University, Alexandria, Egypt.

*** Ph.D., Air Defense College, Alexandria, Egypt.

**** Graduate Student, Air Defense College, Alexandria, Egypt.

1. INTRODUCTION

Early fault detection, diagnosis, and prognosis especially for induction motor, the industrial workhorse, have grasped the attention of many authors. It became essential to detect the fault, isolate it, find the cause, and estimate the new performance and the remaining lifetime of the motor. Model-based fault-detection techniques can be used simultaneously to detect faults in the actuators, process and sensors by measuring input signals and output signals, which usually are contaminated by disturbances. Assuming that the overall process model agrees with the real process including actuators and sensors, faults which change the transfer behavior will lead to changes of the features, calculated by the model-based fault-detection method. However, three basic methods are distinguished for model-based fault detection, parameter estimation, observers and state estimation and parity equations. All methods are applicable to linear and special types of nonlinear processes. A detailed description of these methods is illustrated in [1].

2. CLASSIFICATION OF FAULT-DETECTION METHODS BASED ON MEASURED SIGNALS

Fault-detection methods based on measured signals can be classified into:

- Limit value checking (threshold, tolerances) and plausibility checks (ranges) of single signals.
- Signal model-based methods for single periodic or stochastic signals.
- Process model-based methods for two and more related signals.

3. STATOR FAILURE CAUSES AND ANALYSIS

The majority of stator failures in squirrel-cage induction motors are caused by a combination of various stresses, electrical, mechanical, environmental and thermal. To discuss the relation between the various stresses and how do they affect the life of the stator and contribute to premature failure is given in [2] [3] [4]. There are five key areas that should be considered and related to one another in order to accurately diagnose the cause of stator failures, these are failure mode, failure pattern, appearance, application consideration and maintenance history .[5] [6] [7].

4. BEHAVIOR OF INDUCTION MOTOR DURING STATOR FAILURE

Only one type of stator fault in one instant per phase is considered, healthy rotor and mechanical parts of motor are assumed.[8] [9]

4.1. Turn-to-Turn fault [7]

This type of failure is caused by an insulation breakdown between two turns in the same phase. It has the same effect as a shading coil inserted into the winding. As high current (several times higher than normal current) arises in this coil, the magnetic field produced in this shading coil affects the total magnetic flux in this phase. Turn-to-turn failure in phase *a* is now assumed. The voltage equation for phase *a* are given by:

$$\bar{v}_a = R_a \bar{i}_a + \frac{d\bar{\Psi}_a}{dt} \quad (1)$$

The total flux linking phase a is

$$\bar{\Psi}_a = \bar{\Psi}_{sa} + \bar{\Psi}_{Ra} \quad (2)$$

Where ($\bar{\Psi}_{sa}$) is the flux caused by stator current, ($\bar{\Psi}_{Ra}$) is the flux caused by rotor currents, and is given by:

$$\Psi_{sa} = L_{sa} i_a + M_{ab} i_b + M_{ac} i_c \quad (3)$$

$$\bar{\Psi}_{Ra} = M_{aA} \bar{i}_A + M_{aB} \bar{i}_B + M_{aC} \bar{i}_C \quad (4)$$

Where (L_{sa}) is the self-inductance of phase a, (M_{ax}), is the mutual inductance between phase (a) and x. In the case of turn-to-turn fault in phase a, the magnetic flux produced by shading coil will weaken the total magnetic flux Ψ_a in the phase a. The time derivative of Ψ_a will be lower, voltage drop across the resistance R_a will be higher. Moreover the value of R_a will decrease as a consequence of turn-to-turn fault, but this change has a negligible effect on the voltage. Hence, the result of a turn-to-turn fault in stator phase (a) will be an increase of current I_a . The change of current I_a cause's change of magnetic flux linking the stator phases. The total flux linking phase b and c are such that.

$$\Psi_b = \Psi_{sb} + \Psi_{Rb}, \Psi_c = \Psi_{sc} + \Psi_{Rc}.$$

If there is no changes of rotor current symmetry during any stator failure then,

$$\Psi_{Ra} = \Psi_{Rb} = \Psi_{Rc}, \Psi_{sb} = L_{sb} i_b + M_{ab} i_a + M_{bc} i_c, \Psi_{sc} = L_{sa} i_c + M_{ac} i_a + M_{bc} i_b,$$

The current I_a clearly affects fluxes in phase b and c through the mediation of the mutual inductances. The change of I_a brings the change of magnetic fluxes in the adjacent phases as next step. It depends on the phase order where the magnetic flux becomes higher and where it becomes lower. The nature of this phenomenon is given by a spatial distribution of stator winding. Demonstration and explanation of such behavior of induction motor can be done using phasor diagrams. These diagrams would not describe the exact situation inside the motor, but they will be very useful for a better understanding of the phase currents changes during stator failures. As three-phase set of currents in a stator can produce, a rotating magnetic field can produce three-phase set of voltages in the stator coils. The equations governing the induced voltages in the stator will be developed in this section. Starting with equations (1)-(4) and using phasors instead of instantaneous values.

Rotor magnetic flux linked with phase (a) is constant, therefore the voltage induced in the stator due to this flux is also constant (\bar{v}_{ra})

$$\frac{d\bar{\Psi}_a}{dt} = \frac{d\bar{\Psi}_{Sa}}{dt} + \frac{d\bar{\Psi}Ra}{dt} = L_{Sa} \frac{d\bar{i}_a}{dt} + M_{ab} \frac{d\bar{i}_b}{dt} + M_{aC} \frac{d\bar{i}_c}{dt} + \bar{V}_{iRa} = \bar{V}_{iSaa} + \bar{V}_{iSab} + \bar{V}_{iSaC} + \bar{V}_{iRa}$$

$$\bar{V}_a = R_a \bar{I}_a + \bar{V}_{iSaa} + \bar{V}_{iSab} + \bar{V}_{iSaC} + \bar{V}_{iRa} \quad (5)$$

From the above equations, one is able to construct the phasor diagram as shown in Fig. 1. The phasor diagram of healthy motor is shown in Fig. 1. Phasors diagrams corresponding to different stator faults are shown in Fig. 2. The change of the phasor diagram due to faults as seen can be taken as a measure to predict the onset of faults. This appears in the form of current change in one phase with respect to other phases.

The stator inductances are related as,

$$\frac{M_{ab}}{L_{Sa}} = \frac{M_{aC}}{L_{Sa}} = \frac{1}{k}, \text{ Where } k > 1 \text{ and depends on the stator construction and winding}$$

distribution. For healthy motors, $|\bar{V}_{iSaa}| = k|\bar{V}_{iSab}| = k|\bar{V}_{iSaC}|$.

Consider the same phase voltages even for a faulty stator. (This is not true in real motor there will be a node- shift in the case of stator fault.), The phasors of phase a Fig. 2. ($\cos\phi = 0.7$), illustrate the changes of phasor diagram due to faults. It is important to know that these diagrams are not accurate. We ignore the change of currents phase shift during the stator fault; therefore, voltage drop $R_a I_a$ is not perpendicular to the induced voltage \bar{V}_{iSaa} for the faulty stator on Fig. 2(b, c, d). These diagrams are only used to explain the influence of current change in one phase to currents in other phases.

Figure (2a-d). Shows how the change of current in one phase (a, b or c) can influence the change of induced voltages (according to equation (5)) and consequently the change of voltage drop across R_a . The rotor currents are assumed symmetrical and balanced in the case of a stator failure. Therefore, the induced voltage \bar{V}_{iRa} will be balanced. The change of stator currents phase shift is ignored. This assumption is not real but it allows easier explanation of the nature of current changes in the phases due to stator failure.

Figure (2b) shows the change of induced voltages in phase a after the increase of current I_a (due to a turn-to-turn fault in phase a). The induced voltage \bar{V}_{iSaa} will be higher (due to self- inductance of phase a). The sum of the induced voltages vectors equation (5) will change. The end of the induced voltage vector \bar{V}_{iSaC} will shift to other position in the phasor diagram. The voltage drop $R_a I_a$ will be increase and therefore stator current I_a will be increased too. (Position of vectors in the case of healthy motor is marked by the dotted lines).

Figure (2c). Shows the situation in the phase a after increase of I_b due to a turn-to-turn fault in the phase b. In this case, the induced voltage \bar{v}_{isab} will increase. The voltage drop $R_a I_a$ will also increase and therefore current I_a will increase.

Figure (2d). Shows the change of vector \bar{v}_{isca} due to turn-to-turn fault in phase c (increase of current I_c) resulting in decrease of current I_a .

The behavior of induction motor in case of a turn-to-turn fault described in the figures (2a-d) is valid not only for a given load condition $\cos\phi=0.7$ but for an arbitrary load [7].

If a turn-to-turn fault occurs a higher unbalanced 3-phase, current will be drawn by induction motor from the power supply. The highest current will flow through the faulty phase. For the currents in the two adjacent phases, and the same phase order illustrated in the Fig. 2. we can formulate the following tendencies for the stator currents increasing and decreasing:

Table 1. shows the change of phase currents associated with the turn to turn fault in phases A, B and C.

4.2. Phase-to-Phase fault

A phase-to-phase fault occurs when a short-circuit rises between two different stator phases. This failure has very similar effect as if two turn-to-turn faults in phase a and b in one instant have occurred. In both shading, coils raise in the magnetic fluxes causing a relative current increase or decrease in the adjacent phases (as the previous turn-to-turn fault). However, the situation is now more complex. There can be different types of phase-to-phase fault differing in the position of a short-circuit. [7]

4.3. Phase-to-ground fault [7]

A phase-to-ground fault will break when a short-circuit between a phase and grounded motor frame occurs. In consequence of this fault the currents will leak through the ground and the stator current will not be balanced anymore.

5. Causal Model of induction Motor for Stator Diagnosis[7]

The diagnosis indicates which parts of the system are healthy and which are faulty. This information can be used to generate alerts, to schedule reparations, and to estimate operability of the system. The tool uses symbolic qualitative variables, derived during testing and measurement phases. Real physical quantitative values are classified into qualitative values. The system is able to use these information and to devise the possible combination of component modes

5.1. Measured Variables (observables)

The diagnosis system measures values of the three-phase stator currents. $i_a(t), i_b(t), i_c(t)$.

The effective values of stator currents are I_a, I_b, I_c . the effective value of current in the center of 'Y' winding is denoted I_0 . In case of delta winding or if the center of 'Y' is not accessible, The value of I_0 may be evaluated as[7]

The mapping of the relative quantitative values to the qualitative values. Is done according to Table 1. The variables (CURRENT_S_A, CURRENT_S_B, and CURRENT_S_C) have three qualitative values: LOW, NORMAL, and HIGH are shown in Table 2.

The variable CURRENT_S_SUM has two qualitative values ZERO and NONZERO defined in Table 3.

The last observable used in the model is PHASE_ORDER. It defines the direction of rotation of the stator magnetic field. This variable has two qualitative values: ABC and ACB

5.1.2. System modes (assumables)

The output of the CNETS algorithm is a diagnosis, which is a logical sentence built of assumables. The assumable is a logical variable that represents a health state of a component in the causal model. There is only one assumable in our model that represents health of stator.

Currently, it has (10) qualitative values:

- STATOR_HEALTH= OK - no fault
- STATOR_HEALTH -TURN_F_A - turn-to-turn fault in phase A.
- STATOR_HEALTH -TURN_F_B - turn-to-turn fault in phase B.
- STATOR_HEALTH -TURN_F_C - turn-to-turn fault in phase C.
- STATOR_HEALTH -PHASE_F_AB - phase-to-phase fault between phases A and B.
- STATOR_HEALTH -PHASE F_AC - phase-to-phase fault between phases A and C.
- STATOR_HEALTH -PHASE F_BC - phase-to-phase fault between phases B and C.
- STATOR_HEALTH -GROUND_F_A - ground fault in phase A
- STATOR_HEALTH -GROUND_F_B - ground fault in phase B
- STATOR_HEALTH -GROUND_F_C- ground fault in phase C

5.2. Causal Relationships

Based on the assumptions presented in the above points, the causal relationships between stator faults and qualitative values of stator currents. can be obtained [7].

6. CASE STUDY [10]

In what follows we extended the use of the above procedure to the prediction of faults in the stator of a squirrel-cage induction motors.

6.1 Special Induction Motor for Fault Emulation

For different stator fault emulations the squirrel-cage induction motor, with the following parameters was used. Nominal power (0.37 kW- 0.5 hp), Voltage (380Y/220 D ac V), Current (1.3/2.3A ac), Frequency (50 Hz) and Nominal speed (1400 rpm).

6.2 Stator Faults Emulation

Different types of stator faults were emulated. Turn-to-turn, phase-to-phase and phase-to-ground. The experimental measurement results are given in the following tables. Where, a color background was used for a qualitative value indication. The qualitative values were determined according to the following rules:

Dark blue color		-HIGH (1.1; ∞ >
Light blue color		-NORMAL <0.9; 1.1 >
None background (white)		-LOW <0; 0.9

If a neutral current (I_0) qualitative value (zero or nonzero) is clear, no background was used for this quantity. The first column in the tables contains a name of a data file. The second column brings the information about the type of fault; the third column contains the line current (measured RMS value).

6.2.1 No fault condition

# measurement	Fault type	Ia[A]	Ib[A]	Ic[A]	I line [A]	IO [A]	Ia[-]	Ib[-]	Ic[-]	Io[-]
		Line current (measured,RMS)			AVG value	Neutral curr. (calculated)	p.u.of measured current in relation to actual AVG value			
G0	No fault	1.30	1.30	1.31	1.30	0.04	1.00	1.00	1.00	0.03
G01	No fault	1.31	1.33	1.39	1.34	0.04	0.98	0.99	1.04	0.03
G02	No fault	1.25	1.20	1.25	1.23	0.04	1.01	0.97	1.02	0.03
G03	No fault	1.20	1.26	1.25	1.24	0.04	0.97	1.02	1.01	0.03
G04	No fault	1.27	1.22	1.27	1.25	0.04	1.01	0.97	1.02	0.03

.6.2.2 Turn-To-Turn fault

# measurement	Fault type	I _a [A]	I _b [A]	I _c [A]	I _{line} [A]	I ₀ [A]	I _a [-]	I _b [-]	I _c [-]	I ₀ [-]
		Line current (measured, RMS)			AVG value	Neutral current (calculated)	p.u.of measured current in relation to actual AVG value			I ₀
G1	1A+2A	1.31	1.3	1.3	1.3	0.03	1.01	1.00	1.00	0.02
G2	1A+5A	1.4	1.3	1.3	1.33	0.03	1.05	0.98	0.98	0.02
G3	1A+10A	1.45	1.33	1.2	1.32	0.03	1.10	1.01	0.91	0.02
G4	1A+20A	1.5	1.4	1.2	1.37	0.03	1.10	1.02	0.87	0.02
G5	1A+40A	1.7	1.6	1.1	1.47	0.03	1.16	1.09	0.75	0.02
G6	1A+80A	1.8	1.7	1.1	1.53	0.03	1.18	1.11	0.72	0.02
G7	1A+120A	2.35	2.1	1.2	1.88	0.03	1.25	0.99	0.64	0.02
G8	1A+160A	2.9	2.5	1.3	2.23	0.03	1.30	1.12	0.58	0.01
G9	1A+240A	4.3	3.0	1.8	3.03	0.03	1.30	1.12	0.59	0.01
G10	1A+320A	5.9	3.5	2.2	3.87	0.03	1.52	0.90	0.57	0.01
G11	1B+2B	1.3	1.31	1.3	1.30	0.03	1.00	1.01	1.00	0.02
G12	1B+5B	1.3	1.4	1.3	1.33	0.03	0.98	1.05	0.98	0.02
G13	1B+10B	1.25	1.45	1.3	1.33	0.03	0.94	1.09	0.98	0.02
G14	1B+20B	1.2	1.51	1.42	1.38	0.03	0.87	1.09	1.02	0.02
G15	1B+40B	1.11	1.71	1.62	1.48	0.03	0.75	1.16	1.09	0.02
G16	1B+80B	1.1	1.8	1.7	1.53	0.03	0.72	1.18	1.11	0.02
G17	1B+120B	1.2	2.35	2.1	1.88	0.03	0.64	1.25	1.12	0.02
G18	1B+160B	1.31	2.9	2.53	2.25	0.03	0.58	1.29	1.12	0.01
G19	1B+240B	1.8	4.33	3.1	3.08	0.03	0.58	1.40	1.01	0.01
G20	1B+320B	2.2	5.91	3.6	3.90	0.03	0.56	1.51	0.92	0.01
G111	1C+2C	1.3	1.3	1.3	1.3	0.03	1.00	1.00	1.00	0.02
G112	1C+5C	1.3	1.3	1.4	1.33	0.03	0.98	0.98	1.05	0.02
G113	1C+10C	1.4	1.2	1.45	1.35	0.03	1.04	0.89	1.07	0.02
G114	1C+20C	1.4	1.2	1.5	1.37	0.03	1.02	0.87	1.09	0.02
G115	1C+40C	1.61	1.11	1.7	1.47	0.03	1.10	0.76	1.16	0.02
G116	1C+80C	1.7	1.1	1.81	1.54	0.03	1.10	0.71	1.17	0.02
G117	1C+120C	2.0	1.2	2.34	1.85	0.03	1.08	0.65	1.26	0.02
G118	1C+160C	2.52	3.1	2.92	2.85	0.03	0.88	1.09	1.02	0.01
G119	1C+240C	3.12	1.83	4.31	3.08	0.03	1.01	0.59	1.39	0.01
G110	1C+320C	3.66	2.3	5.92	3.96	0.03	0.92	0.58	1.64	0.01

7. NEURAL BASED DIAGNOSIS [10]

In this section, we introduce our proposed method for diagnosis based upon the artificial neural network. It makes use of the algorithms described above. Results of training are shown in Fig. 3. The algorithm has proven adequacy in predicting stator faults with the advantage of simplicity, efficiency and time saving. The algorithm is also extendable to rotor faults with minor modifications.

8. CONCLUSIONS

in this paper a neural based algorithm for detecting stator faults in the three-phase squirrel-cage induction motor presented. The algorithm is based on both qualitative and quantitative measures for diagnoses. The neural network architecture is simple and adequate.

REFERENCES

- [1] Balle, P. and Isermann, "Trends in The Application of Model-Based Fault Detection and Diagnosis of Technical Processes", Control Engineering Practice, vol. 5, no.5, PP.709-719, 1997
- [2] W. T. Martiny, R. Dey, and H. B. Margolis, "Thermal Relationship in an Induction Motor Under Normal and Abnormal Operation,"AIEE Trans. Power App. Syst., vol. pas-80. Pp.66- 78, Apr. 1961.
- [3] A.H.Bonnett and G.C. Soukup,"Analysis of Winding Failures in Three-Phase Squirrel-Cage Induction Motors,"IEEE Trans. Ind. Applicat., vol. IA-14, no.3, pp223-226, May/June1978.
- [4] A.H. Bonnett and G.C. Soukup,"Causes and Analysis of Stator and Rotor Failures in Three-Phase Squirrel-Cage Induction Motors,"IEEE Trans.Ind.Applicat., vol.28 pp .921- 937, July/Aug. 1992.
- [5] S. Williamson and K. Mirzoian, "Analysis of Cage ind. Motors with stator winding Faults, "in Proc. IEEE-PAS Annu. Meeting, July 1985, vol. 104, pp. 1838-1842.
- [6] S. Nandi, and H. A. Toliyat, "Performance analysis of a three phase induction motor under abnormal operating conditions", presented in IEEE-SDEMPED, 1997.
- [7] Petr Kadanik, O. Cervinka, Jiri Ryba.: Causal Model of Induction Motor for Stator Diagnostics, Praha 2000, Research Report, Rockwell Automation AT Prague Labs.
- [8] Ryba, J.: Induction motor diagnostics, Praha 1997, Research Report, Rockwell Automation AT Prague Labs.
- [9] Hejda, P.-Cervinka, O.: CNET Manual, Praha 1999, Research Report, Rockwell Automation AT Prague Labs.
- [10] G. Mahmoud: fault detection for induction motors by signature analysis, Msc. Faculty of Engineering, Alexandria University, 2002.

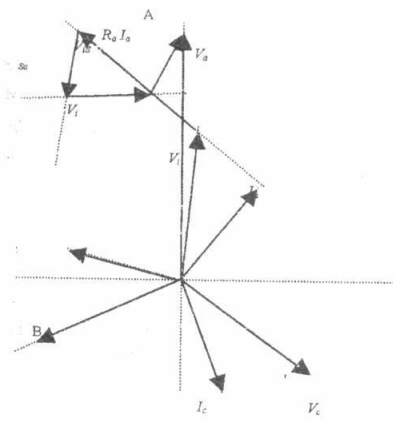


Fig. 1. Phasor diagram for a healthy motor

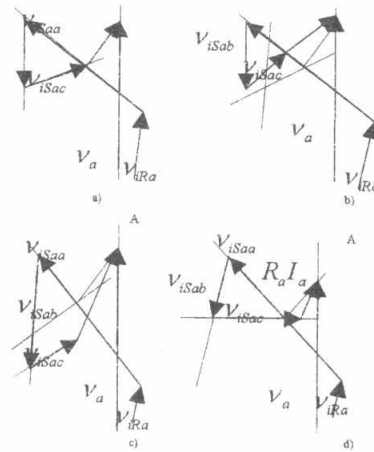


Fig. 2. Simplified detailed phasor diagram of IM (phase a, $\cos\phi = 0.7$) [7]

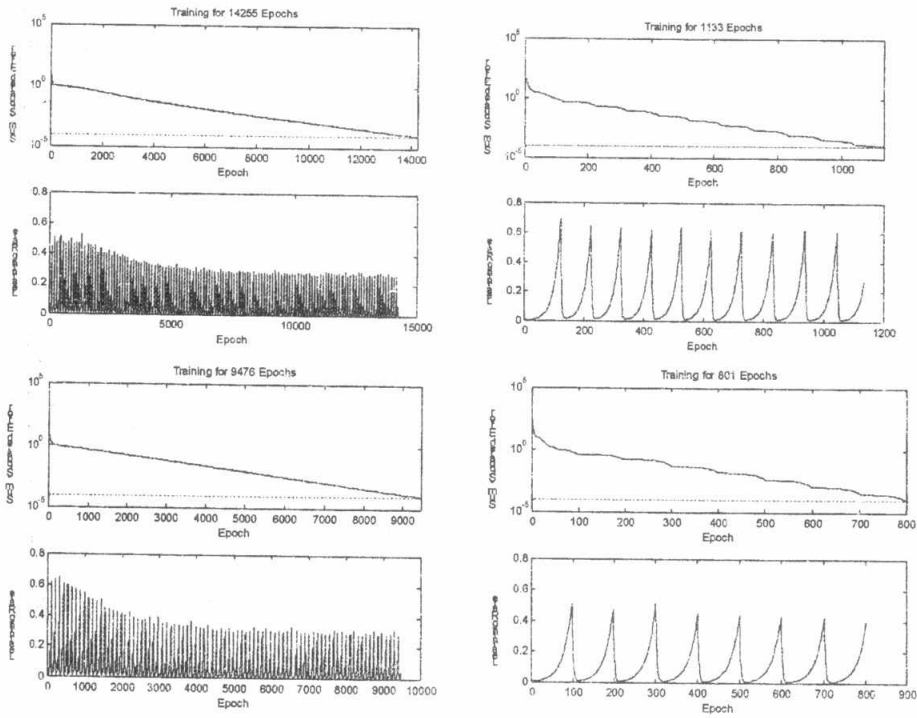


Fig. 3. Results of Training the Neural-Networks

Table 1. Relative changes of stator currents caused by turn-to-turn faults[7]

Fault Type	Relative change of a phase current		
	Phase a	Phase b	Phase c
Turn-to-turn in phase A	Increase ↑↑	Decrease ↓	Increase ↑
Turn-to-turn in phase B	Increase ↑	Increase ↑↑	Decrease ↓
Turn-to-turn in phase C	Decrease ↓	Increase ↑	Increase ↑↑

Table 2. The qualitative values of the stator current

Relative (quantitative) value	Qualitative value
< 0 ; 0.9) <0.9;1.1> (1.1;<»)	LOW NORMAL HIGH

Table 3. The qualitative values of the stator current (CURRENT_S_SUM)

Relative (quantitative) value	Qualitative value
< 0;0.1 > (0.1 ; ∞)	ZERO NONZERO